JACS
JOURNAL OF THE AMERICAN CHEMICAL SOCIETY

COMMUNICATION

pubs.acs.org/JACS

Exploring Organosilane Amines as Potent Inhibitors and Structural Probes of Influenza A Virus M2 Proton Channel

Jun Wang,[†,∥] Chunlong Ma,[‡] Yibing Wu,[∥] Robert A. Lamb,[⊥] Lawrence H. Pinto,[‡] and William F. DeGrado*[,†,∥]

[†]Department of Chemistry and [∥]Department of Biochemistry and Biophysics, School of Medicine, University of Pennsylvania, Philadelphia, Pennsylvania 19104-6059, United States

[⊥]Howard Hughes Medical Institute and Department of Biochemistry, Molecular Biology and Cell Biology and [‡]Department of Neurobiology and Physiology, Northwestern University, Evanston, Illinois 60208-3500, United States

Supporting Information

ABSTRACT: We describe the use of organosilanes as inhibitors and structural probes of a membrane protein, the M2 proton channel from influenza A virus. Organosilane amine inhibitors were found to be generally as potent as their carbon analogues in targeting WT A/M2 and more potent against the drug-resistant A/M2-V27A mutant. In addition, intermolecular NOESY spectra with dimethyl-substituted organosilane amine inhibitors clearly located the drug binding site at the N-terminal lumen of the A/M2 channel close to V27.

Influenza A virus is a serious human health threat that urgently requires development of small-molecule antiviral agents.[1] Drug resistance is the predominant issue in influenza pharmaceutical research, due to the rapid mutational rate and high tendencies toward reassortment.[2] Currently, there are four small-molecule drugs used for the prevention and treatment of influenza A virus infections in the United States. Oseltamivir and zanamivir are neuraminidase inhibitors that block the release of progeny viruses from the host cells; amantadine and rimantadine are M2 channel blockers that inhibit the viruses' uncoating process by preventing the acidification of endosomally entrapped viruses. However, most currently circulating viruses are resistant to amantadine and rimantadine, and the number of viruses resistant to oseltamivir and zanamivir is on the rise.[3] Thus, there is clearly a need to develop novel antivirals that are able to combat drug-resistant viruses.

A/M2 forms a homotetrameric proton-selective channel in viral membranes and plays an essential role in mediating viral uncoating[4] and budding.[5] Additionally, it equilibrates the pH across the Golgi apparatus to prevent the premature conformational change of hemagglutinin.[6−8] A/M2 is more conserved than other drug targets of influenza A virus, with only three predominant drug-resistant mutations, S31N, V27A, and L26F, observed in widely circulating viruses,[9,10] all of which are located in the transmembrane domain drug binding site.

A carbon-to-silicon switch is a widely explored strategy in developing and marketing organosilane pesticides.[11,12] There is also a continuing interest in the pharmaceutical industry to fine-tune the pharmacological or pharmacokinetic properties of marketed drugs using the same strategy.[13−16] Silicon-containing compounds generally have no heavy metal associated toxicities and have metabolic profiles similar to those of their carbon analogues.[13,14] Apart from the increased size and hydrophobicity of silicon compared to the corresponding carbon counterpart, organosilanes can also be designed to mimic high-energy tetrahedral intermediates or novel scaffolds that are not accessible to carbon analogues.[17,18] The most common carbon-to-silicon switch strategies fall into one of the two classes (Scheme 1). In the first class, a quaternary carbon is replaced with a silicon to increase hydrophobicity[19] (Scheme 1a). In the second class, a carbonyl is replaced with a sterically hindered silanediol to mimic the high-energy intermediate of an amide-bound hydrolysis, providing opportunities to inhibit proteins such as proteases[20] (Scheme 1b).

Scheme 1. Common Strategies of Carbon-to-Silicon Switch in Drug Design[a]

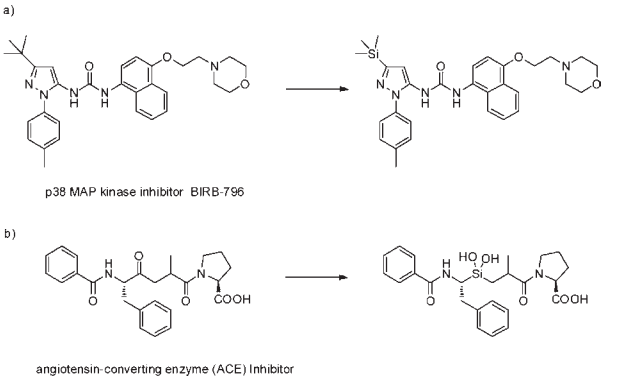

[a] In path a, *tert*-butyl is substituted by trimethylsilane in p38 MAP kinase inhibitor; in path b, silanediols were designed to mimic the tetrahedral hydrolysis intermediate in ACE inhibitor.

Hydrophobicity plays a critical role in improving antiviral potency in designing A/M2 inhibitors as anti-influenza drugs.[21−23] The pore-facing residues of the A/M2 channel (V27, A30, S31, and G34)[24,25] form a hydrophobic binding pocket that favors binding of hydrophobic molecules such as adamantane or spirane amines. Our previous structure−activity relationship (SAR) studies of spirane amine compounds showed a positive correlation between hydrophobicity and antiviral potency.[22,23] Considering the increased size and hydrophobicity of silicon compared with its carbon analogue, we therefore rationalized that replacement of the quaternary carbon in spirane amine inhibitors with silicon would increase their potency.

Received: June 1, 2011
Published: August 05, 2011

1 2

Figure 1. The smallest known organic M2 inhibitor.

Scheme 2. Synthesis of Silaspirane Amines

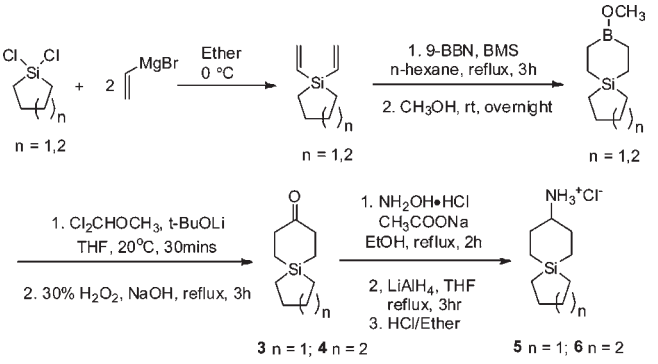

Another interesting aspect of organosilane compounds is that C−Si bond is polarized toward carbon due to the higher electronegativity of carbon (2.50 for carbon and 1.74 for silicon). This results in an upfield chemical shift of silicon α-protons to ~0 ppm, which is generally well separated from the protein background signals. In light of this unique property, we envisioned that organosilane compounds can be applied to map the A/M2 channel drug binding site using simple nuclear Overhauser enhancement spectroscopy (NOESY), thereby obviating the need for more technically demanding and less sensitive half-filtered experiments.[26]

The minimal requirements for potent inhibition of A/M2 are a basic group attached to an alkyl moiety of at least eight carbon atoms with good steric fit to the A/M2 binding cavity.[21] To test the effectiveness of a carbon-to-silicon switch in A/M2 inhibitor design, we first examined a commercially available organosilane amine, (3-Aminopropyl)trimethylsilane hydrochloride (**2**, Figure 1), which contains only six carbons and one silicon. Encouragingly, it showed a 75.5 ± 0.5% inhibition against the wild-type (WT) A/M2 at 100 μM concentration in a two-electrode voltage clamp (TEVC) assay, which is comparable with the eight-carbon analogue **1** (86.6 ± 1.1%).[21] This is by far the smallest molecule (less than eight carbons) that is active against A/M2.

In this study, two silaspirane amines, **5** and **6**, were designed and synthesized on the basis of the previously identified spirane amine scaffold (Scheme 2). The synthesis started from dichlorosilane, and double substitution of the chlorides with vinylmagnesium bromide yielded the divinyl cyclosilane.[27,28] Without purification, it underwent hydroboration with 9-borabicyclo[3.3.1]nonane (9-BBN), followed by an exchange reaction with borane−methyl sulfide complex (BMS), and subsequent methanolysis gave the silaborinane intermediate.[29] Next, Brown's dichloromethyl methyl ether (DCME) process and oxidation with 30% H_2O_2 furnished the spirosilicon ketone intermediates, **3** and **4**, in a one-pot process with ~40−50% overall yield.[27,28] Finally, the ketone was converted to amines **5** and **6** using the two-step hydroxylamine condensation/reduction with ~75% yield.[23]

The synthesized inhibitors were tested in a TEVC assay using *Xenopus laevis* frog oocytes micro-injected with RNA expressing either the WT A/M2 or A/M2-V27A mutant protein.[30] The potency of the inhibitors was expressed as the percentage inhibition of A/M2 current observed after 2 min of incubation with 100 μM compounds, and IC_{50} values were determined for selected potent compounds. The results are summarized in Table 1. As discussed previously, the potency in this assay reflects primarily the kinetics of binding rather than true equilibrium due to the difficulty of maintaining the oocytes for extended periods at low pH.[21] Thus, the IC_{50} values reflect upper limits of the true dissociation constant.

Table 1. Antiviral Activities of Silaspirane Amines against WT A/M2 and A/M2-V27A Mutants

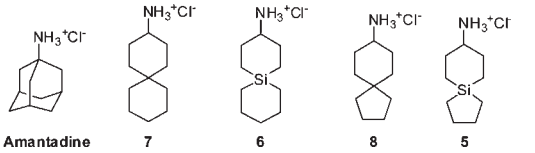

Amantadine 7 6 8 5

	amantadine	7	6	8	5
WT A/M2[a]	90.8 ± 2.5	89.0 ± 1.5	94.5 ± 0.6	95.9 ± 0.9	93.9 ± 1.8
IC_{50} (μM)	16 ± 1.2	12.6 ± 1.1	13.7 ± 1.7	3.3 ± 0.2	7.8 ± 0.6
A/M2-V27A[a]	0	53.2 ± 2.3	67.4 ± 1.1	25.2 ± 0.9	47.8 ± 0.5
IC_{50} (μM)	NA[b]	84.9 ± 13.6	31.3 ± 2.3	318.6 ± 57.3	96.3 ± 13.4

[a] Inhibition (%) at 100 μM inhibitor concentration. [b] NA = not available. All compounds were also tested against S31N mutant and found to have <20% inhibition at 100 μM.

As expected, both silaspirane amines, **6** and **5**, showed potencies similar to those of their carbon analogues, **7** and **8**, in inhibiting WT A/M2 channel activity. All were more active than amantadine. Noteworthy was an increase in antiviral potency of silaspirane amine inhibitors against A/M2-V27A compared to their carbon analogues. The IC_{50} of **6** against A/M2-V27A was 31.1 μM, which is more than 2.7-fold more potent than the previously identified weak A/M2-V27A inhibitor, **7**. Similarly, a 3.3-fold potency increase against the V27A mutant was seen when the quaternary carbon in **8** was switched to silicon to give **5**. The dramatic antiviral potency increase against V27A by switching to silicon might be due to the larger size and higher lipophilicity of silicon compared with carbon, thus providing better hydrophobic contact between the drug and the channel.[31,32]

Membrane proteins are characterized by high content of aliphatic residues (Ala, Val, Leu, Ile),[33] and this results in crowded signal overlap at 0.5−1 ppm in the proton dimension of their NMR spectra; also their large size and rapid relaxation render traditional half-filtered experiments difficult. To map the drug binding sites in membrane proteins, it is desired to have a small-molecule inhibitor which shows characteristic signals beyond the normal range of protein signals. To achieve this goal, two 4,4-disubstituted silacyclohexane amine derivatives (**10** and **14**) and one 4,4-dimethyl-1,4-azasilepane (**13**) were designed and synthesized (Table 2 and Supporting Information (SI) Scheme S1).

4,4-Dimethyl silacyclohexane amines **10** and **14** showed a high potency against the WT A/M2 and only minimal inhibition against A/M2-V27A mutant (Table 2), which was expected, as A/M2-V27A prefers binding molecules with extended conformations.[23,32] Compound **13** was found to be less active than **10** and **14**, but slightly more active than its carbon analogue **16**. The chemical shifts of the methyl protons in all three organosilane amine compounds were close to 0 ppm, which is distinguished from the protein signals and is ideal for them to serve as structural probes for intermolecular NOESY experiments.

With the structural probes (**10**, **14**, and **13**) in hand, we next pursued ^{13}C-edited NOESY spectra with WT M2TM (22−46)

peptide reconstituted in DPC micelles. To facilitate assignment, residues at positions V27, A30, and G34 were selectively, uniformly ^{15}N and ^{13}C labeled. When 2 equiv of compound **10** (1 mM) was added to M2TM tetramer (0.5 mM), two strong NOE cross-peaks were observed between one of the two methyl groups from **10** and both of the γCH_3 groups of V27 (Figure 2b); weaker NOEs were observed for the other methyl group of **10** and both of the γCH_3 groups of V27. This methyl group also shows an NOE to the βCH_3 of Ala30 (Figure 2b). The nonequivalent cross-peaks between the two methyl groups of **10** reflect the nonsymmetrical binding geometry of the drug inside the channel. The substituent with stronger NOE signals to V27 is assigned to the axial methyl from **10**, which in models is closer to V27 than A30;[34,35] the methyl group that showed cross-peaks to Ala30 was assigned to the equatorial methyl from **10**. No NOEs were found between the methyl groups of **10** and Gly34, which lies lower in the structure of the channel as viewed in Figure 2d. This binding model is consistent with our earlier studies showing that the drug binds inside the channel with amine pointing down toward H37 (Figure 2d).[36] The same NOE cross-peak patterns were observed when the experiment was repeated with only 1 equiv of **10** (0.5 mM) (SI Figure S1). In comparison with **10**, the two methyl groups in **13** are equivalent, showing a single peak at 0.07 ppm (indicative of a lower barrier for interconversion of the seven-membered ring). As a weaker inhibitor against WT A/M2 compared with **10**, when 2 equiv (1 mM) of **13** was added to M2TM tetramer (0.5 mM), two strong NOE cross-peaks were observed and assigned to the γCH_3 of V27 and the methyl protons of **13**. In addition, an unambiguous NOE was assigned to the βCH_3 of A30 and the methyl protons of **13** (Figure 2f).

Table 2. Antiviral Activities of Organosilane Structural Probes against WT A/M2 and A/M2-V27A Mutants

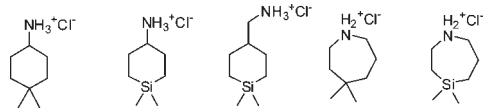

	15	**10**	**14**	**16**	**13**
WT A/M2[a]	95.3 ± 1.1	95.4 ± 1.4	95.4 ± 0.4	75.4 ± 1.8	78.5 ± 1.2
IC_{50} (μM)	2.4 ± 0.2	2.6 ± 0.2	5.7 ± 0.3	26.1 ± 2.2	19.4 ± 1.6
A/M2-V27A[a]	0	7.9 ± 1.1	19.1 ± 1.0	2.5 ± 0.4	0
IC_{50} (μM)	NA[b]	NA	NA	NA	NA

[a] Inhibition (%) at 100 μM inhibitor concentration. [b] NA = not available. All compounds were also tested against S31N mutant and found to have <20% inhibition at 100 μM.

Both **16** and its silicon analogue **13** were crystallized by solvent evaporation in CH_2Cl_2/CH_3OH (3:1 v/v) and their structures determined by X-ray crystallography. The Si−C bond length (1.87 Å) was found to be on average 22% longer than the corresponding C−C bond length (1.54 Å), which results in nearly 50% volume increase at the quaternary center (SI Table S1). The size expansion effect of the carbon-to-silicon switch might contribute to the antiviral potency increase of organosilane against A/M2-V27A, as the expanded organosilane amine is able to fill in the extra space created by the bulky valine 27 to smaller alanine mutation (Table 1). Moreover, silanes are more lipophilic than the corresponding alkanes; the ClogPs for **16** and **13** are 2.99 and 4.15, respectively. Thus, the improved antiviral potency of organosilanes compared with their carbon analogues might be due to the synergetic effects of size expansion and increased lipophilicity.

Biologically active organosilanes, discovered through either rational design or high-throughput screening, are attractive analogues of their carbon counterparts due to their unique properties. Carbon-to-silicon switch retains the overall 3D conformation of the inhibitor, thus providing a minimal perturbation

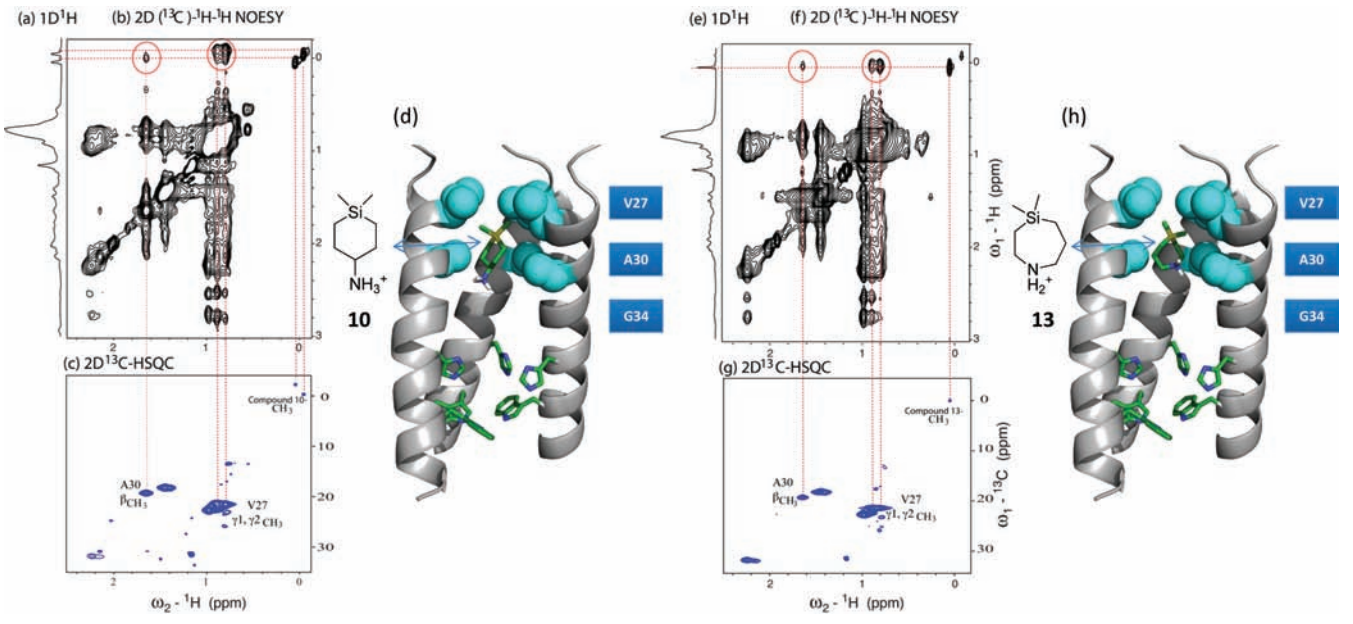

Figure 2. ^{13}C-edited ^1H NOESY spectra of M2TM(22-46)-$V_{27}A_{30}G_{34}$ in DPC micelles in the presence of either **10** (spectra a−c) or **13** (spectra e−g). **10** and **13** are bound in the pore, as assessed from intermolecular NOEs circled in red. (a,e) Upfield region of 1D ^1H NMR. (b,f) Upfield region of 2D ^{13}C-edited ^1H NOESY spectra with 100 ms mixing time. (c,g) Upfield region of 2D ^{13}C-HSQC; complete assignment was reported earlier.[36] (d,h) Docking models of compounds **10** and **13** in the A/M2 channel. The poses of the drugs reflect the relative NOE signal intensities. Sample conditions: 2 mM A/M2(22-46) with residues $V_{27}A_{30}G_{34}$ double-^{15}N,^{13}C-labeled, 100 mM DPC, 1 mM **10** or **13**, and 50 mM pH 7.5 phosphate buffer in 10% D_2O, 90% H_2O. Spectra were recorded at 313 K on a Varian Inova 600 MHz (for **13**) or a Bruker Avance 500 MHz spectrometer (for **10**).

of the binding between the ligand and the receptor. Additionally, the larger covalent radius of silicon (1.17 Å) compared to that of carbon (0.77 Å) (SI Table S1), and the higher hydrophobicity renders the organosilane-based inhibitors with improved properties. Organosilanes are also often easier to synthesize than their carbon analogues and, in certain cases, allow access to novel scaffolds not accessible by standard carbon chemistry.[17] In this report, we explored a carbon-to-silicon switch in A/M2 inhibitors design. The silaspirane amines were as potent as their carbon counterparts against WT and were more potent in targeting drug-resistant V27A, which highlights their promise for further optimization. Moreover, this replacement shows promise for NMR spectroscopy; three organosilane structural probes were designed to map the A/M2 drug binding site. Previously, a debate concerning the location of the pharmacologically relevant A/M2 drug binding site(s) was settled in favor of the pore-binding model using the intermolecular deuterium−^{13}C dipolar dephasing experiments in solid-state NMR[37] as well as the solution NOESY difference experiments.[36] The organosilane structural probes designed in this study provide a direct measurement of NOESY cross peaks between the organosilane drug and the A/M2 protein. The ^{13}C-edited ^{1}H NOESY clearly showed the drug binds inside the A/M2 channel, close to the N-terminal lumen, with its positively charged ammonium pointing down toward His37. In conclusion, our studies not only provide a strategy for improving the potency of A/M2 inhibitors but also demonstrate the utility of organosilanes as structural probes for drug binding site mapping, which can be similarly applied to other proteins. This work shows the potential of using organosilane analogues for direct detection of drug−protein interactions, using the highly sensitive NOESY experiment, thereby alleviating frequently encountered problems associated with half-filtered experiments.

■ ASSOCIATED CONTENT

Supporting Information. Experimental procedures and spectroscopic data. This material is available free of charge via the Internet at http://pubs.acs.org.

■ AUTHOR INFORMATION

Corresponding Author
wdegrado@mail.med.upenn.edu

■ ACKNOWLEDGMENT

This work was supported by the NIH (GM56423 and AI74571). J.W. thanks Dr. Patrick J. Carroll for assistance in obtaining X-ray crystallographic data and Ivan Korendovych, Paul Billing, and Belgin Canturk for fruitful comments on the manuscript. We thank Guy Montelione and Walter Englander for NMR time on the Varian 600 and Bruker 500 MHz NMR spectrometers, respectively.

■ REFERENCES

(1) De Clercq, E. *Nat. Rev. Drug Discov.* **2006**, *5*, 1015–1025.
(2) Nelson, M. I.; Viboud, C.; Simonsen, L.; Bennett, R. T.; Griesemer, S. B.; George, K. S.; Taylor, J.; Spiro, D. J.; Sengamalay, N. A.; Ghedin, E.; Taubenberger, J. K.; Holmes, E. C. *PLos Pathogens* **2008**, *4*, e1000012.
(3) Baz, M.; Abed, Y.; Papenburg, J.; Bouhy, X.; Hamelin, M.-Ã. v.; Boivin, G. *N. Engl. J. Med.* **2009**, *361*, 2296–2297.
(4) Pinto, L. H.; Holsinger, L. J.; Lamb, R. A. *Cell* **1992**, *69*, 517–528.
(5) Rossman, J. S.; Jing, X. H.; Leser, G. P.; Lamb, R. A. *Cell* **2010**, *142*, 902–913.
(6) Grambas, S.; Hay, A. J. *Virology* **1992**, *190*, 11–18.
(7) Sugrue, R. J.; Bahadur, G.; Zambon, M. C.; Hallsmith, M.; Douglas, A. R.; Hay, A. J. *EMBO J.* **1990**, *9*, 3469–3476.
(8) Sakaguchi, T.; Leser, G. P.; Lamb, R. A. *J. Cell. Biol.* **1996**, *133*, 733–747.
(9) Furuse, Y.; Suzuki, A.; Kamigaki, T.; Oshitani, H. *Virol. J.* **2009**, *6*.
(10) Furuse, Y.; Suzuki, A.; Oshitani, H. *Antimicrob. Agents Chemother.* **2009**, *53*, 4457–4463.
(11) Sieburth, S. M.; Langevine, C. N.; Dardaris, D. M. *Pestic. Sci.* **1990**, *28*, 309–319.
(12) Sieburth, S. M.; Manly, C. J.; Gammon, D. W. *Pestic. Sci.* **1990**, *28*, 289–307.
(13) Bains, W.; Tacke, R. *Curr. Opin. Drug Discovery Dev.* **2003**, *6*, 526–543.
(14) Showell, G. A.; Mills, J. S. *Drug Discov. Today* **2003**, *8*, 551–556.
(15) Mills, J. S.; Showell, G. A. *Exp. Opin. Invest. Drugs* **2004**, *13*, 1149–1157.
(16) Pooni, P. K.; Showell, G. A. *Mini-Rev. Med. Chem.* **2006**, *6*, 1169–1177.
(17) Voronkov, M. G. *Top. Curr. Chem.* **1979**, *84*, 77–135.
(18) Black, C. A.; Ucci, J. W.; Vorpagel, J. S.; Mauck, M. C.; Fenlon, E. E. *Bioorg. Med. Chem. Lett.* **2002**, *12*, 3521–3523.
(19) Barnes, M. J.; Conroy, R.; Miller, D. J.; Mills, J. S.; Montana, J. G.; Pooni, P. K.; Showell, G. A.; Walsh, L. M.; Warneck, J. B. H. *Bioorg. Med. Chem. Lett.* **2007**, *17*, 354–357.
(20) Sieburth, S. M.; Nittoli, T.; Mutahi, A. M.; Guo, L. X. *Angew. Chem., Int. Ed.* **1998**, *37*, 812–814.
(21) Wang, J.; Ma, C.; Balannik, V.; Pinto, L. H.; Lamb, R. A.; DeGrado, W. F. *ACS Med. Chem. Lett.* **2011**, *2*, 307–312.
(22) Wang, J.; Cady, S. D.; Balannik, V.; Pinto, L. H.; DeGrado, W. F.; Hong, M. *J. Am. Chem. Soc.* **2009**, *131*, 8066–8076.
(23) Balannik, V.; Wang, J.; Ohigashi, Y.; Jing, X. H.; Magavern, E.; Lamb, R. A.; DeGrado, W. F.; Pinto, L. H. *Biochemistry* **2009**, *48*, 11872–11882.
(24) Stouffer, A. L.; Acharya, R.; Salom, D.; Levine, A. S.; Di Costanzo, L.; Soto, C. S.; Tereshko, V.; Nanda, V.; Stayrook, S.; DeGrado, W. F. *Nature* **2008**, *452*, 380–380.
(25) Acharya, R.; Carnevale, V.; Fiorin, G.; Levine, B. G.; Polishchuk, A. L.; Balannik, V.; Samish, I.; Lamb, R. A.; Pinto, L. H.; DeGrado, W. F.; Klein, M. L. *Proc. Natl. Acad. Sci. U.S.A.* **2010**, *107*, 15075–15080.
(26) Zwahlen, C.; Legault, P.; Vincent, S. J. F.; Greenblatt, J.; Konrat, R.; Kay, L. E. *J. Am. Chem. Soc.* **1997**, *119*, 6711–6721.
(27) Soderquist, J. A.; Shiau, F. Y.; Lemesh, R. A. *J. Org. Chem.* **1984**, *49*, 2565–2569.
(28) Soderquist, J. A.; Negron, A. *J. Org. Chem.* **1989**, *54*, 2462–2464.
(29) Damour, D.; Renaudon, A.; Mignani, S. *Synlett* **1995**, 111–112.
(30) Balannik, V.; Lamb, R. A.; Pinto, L. H. *J. Biol. Chem.* **2008**, *283*, 4895–4904.
(31) Pielak, R. M.; Chou, J. J. *Biochem. Biophys. Res. Commun.* **2010**, *401*, 58–63.
(32) Wang, J.; Ma, C.; Fiorin, G.; Carnevale, V.; Wang, T.; Hu, F.; Lamb, R. A.; Pinto, L. H.; Hong, M.; Klein, M. L.; DeGrado, W. F. *J. Am. Chem. Soc.* **2011**, *133*, 12834–12841.
(33) Luckey, M., *Membrane Structural Biology: With Biochemical and Biophysical Foundations*, 1st ed.; Cambridge University Press: Cambridge, UK, 2008.
(34) Aliev, A. E.; Harris, K. D. M. *J. Am. Chem. Soc.* **1993**, *115*, 6369–6377.
(35) Arnason, I.; Kvaran, A.; Jonsdottir, S.; Gudnason, P. I.; Oberhammer, H. *J. Org. Chem.* **2002**, *67*, 3827–3831.
(36) Cady, S. D.; Wang, J.; Wu, Y.; DeGrado, W. F.; Hong, M. *J. Am. Chem. Soc.* **2011**, *133*, 4274–4284.
(37) Cady, S. D.; Schmidt-Rohr, K.; Wang, J.; Soto, C. S.; DeGrado, W. F.; Hong, M. *Nature* **2010**, *463*, 689–692.